EC4MACS

Modelling Methodology

The CHIMERE Atmospheric Model

European Consortium for Modelling of Air Pollution and Climate Strategies - EC4MACS

Editors:

Bertrand BESSAGNET

Etienne TERRENOIRE

Frédéric TOGNET

Laurence ROUÏL

Augustin COLETTE

Laurent LETINOIS

Laure MALHERBE

Issued by: INERIS

March 2012

ABSTRACT

The CHIMERE chemistry transport model is used in the frame of EC4MACS to add the urban dimension in the integrated assessment model GAINS. The CHIMERE model configured for EC4MACS is described in this report. The main improvements implemented in CHIMERE are related to the **meteorology** (Kz and wind speed corrections), **the vertical resolution** (add of a thin first layer, 20 m, at the ground level) and the **emissions** (improvement of the spatialisation and temporal distribution of SNAP2 emissions).

A comprehensive evaluation of the CHIMERE model was conducted for the year 2009. The performance of the model is varying according to the typology of stations and the seasons. CHIMERE reproduces nicely the day to day O3 variation similarly at urban and rural sites with an overestimation which is higher during the winter at urban sites. **CHIMERE gives an overall satisfactory performance for the simulation of the PM10 concentrations and a good performance concerning the simulation of PM2.5 concentrations**. For sulphate, the model performs rather well during the summer but overestimates the concentration at spring time. The modelled nitrate concentrations exhibit a systematic bias that is due to the missing coarse nitrate fraction. The total ammonia is better reproduced by the model during spring and autumn whereas the model performance is lower during the summertime. CHIMERE reproduces the daily NO2 variability along the year but underestimates significantly the concentration especially during the cold season. The PM are still underestimated by the model over the East part of Europe in winter, underestimation of emissions is probably the main reason for such a remaining behaviour. However the main added-value of the new CHIMERE model developed for EC4MACS is that the overall performances in terms of PM concentrations in urban areas are now amongst the best ones, considering regional chemistry transport models available in Europe. The statement that the missing part in PM concentration should be mainly due to missing emissions of particles and their precursors can be accepted.

TABLE OF CONTENT

1 Introduction and context

The CHIMERE chemistry transport model is used in the frame of EC4MACS to add the urban dimension in the integrated assessment model GAINS. Currently, GAINS is fed by source matrix receptors computed with coarse model outputs from the EMEP[1] chemistry transport model (CTM). The former City-Delta project brought together the 17 major European urban and regional scale atmospheric dispersion models (Thunis et al., 2007) and developed a generalized methodology to describe the increments in PM2.5[2] concentrations in urban background air that originate - on top of the long range transport component - from local emission sources. These relationships associate the difference in the annual mean PM2.5 concentrations between an urban area and the average concentrations calculated over the 50 km x 50 km grid cell surrounding the city with spatial variations in emission densities of low-level sources and city-specific meteorological and topographic factors. This relation is currently in use in GAINS (Amann et al., 2011). The objective of the EC4MACS methodology is to add an innovative downscaling methodology in GAINS to improve the assessment of emission reduction strategies for air quality standards compliance (Figure 1). In this report, we will focus on NO2 and PM (Particulate Matter) concentrations since urban areas are the locations where their limit values are generally exceeded in Europe. Regulatory limit values and air quality objectives according to the European Directives are summarised in the Table 1.

Table 1 : PM10 and NO2 standards

Pollutant	***Concentration***	***Averaging period***	***Legal nature***	***Number of exceedances permitted each year***
PM10	50 µg/m^3	24 hours	Limit value entered into force 1.1.2005	35
	40 µg/m^3	1 year	Limit value entered into force 1.1.2005	NA
NO2	200 µg/m^3	1 hour	Limit value entered into force 1.1.2010	18
	40 µg/m^3	1 year	Limit value entered into force 1.1.2010	NA

[1] The EMEP models have been instrumental to the development of air quality policies in Europe since the late 1970's, mainly through their support to the strategy work under the Convention on Long-range Transboundary Air Pollution. In the 1990s the EMEP models became also the reference tools for atmospheric dispersion calculations as input to the Integrated Assessment Modelling, which supports the development of air quality polices in the European Union. While results from the EMEP models have been available to the international community through the EMEP programme for many years, the model code of one of the EMEP chemical transport models was made publicly available only recently.

[2] Mass concentration of particles having a diameter below 2.5 µm

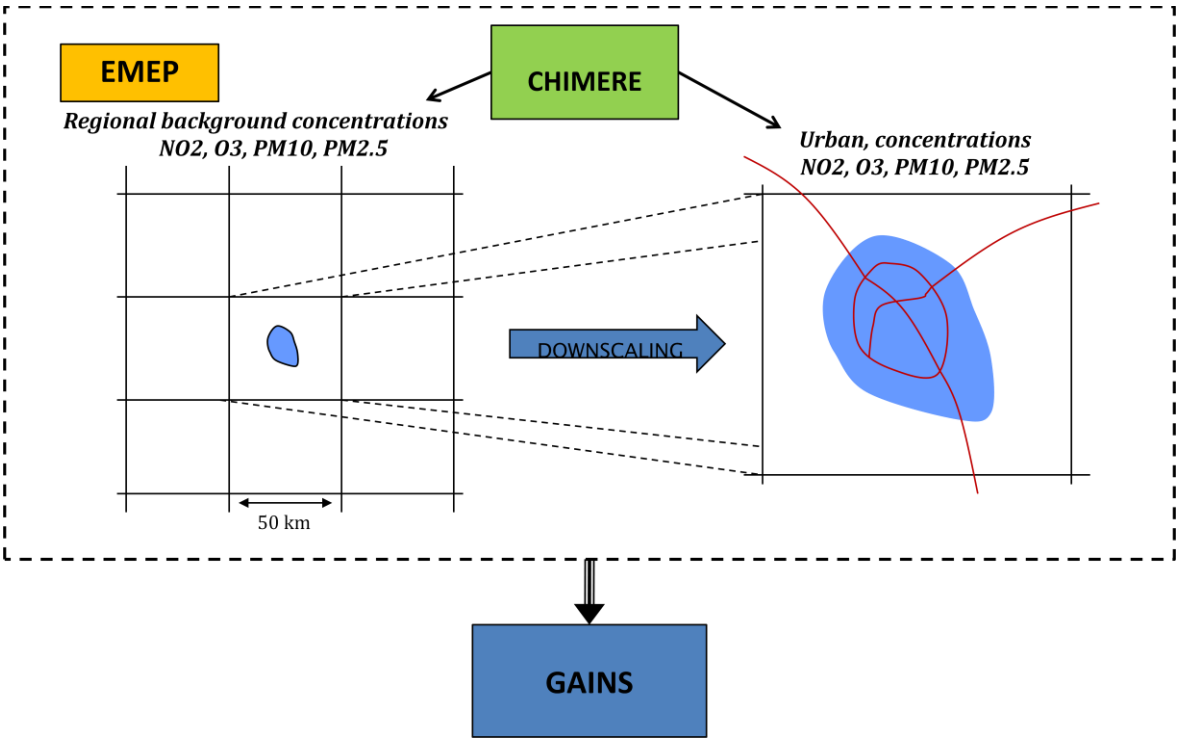

Figure 1 : EMEP background outputs as input data for GAINS. The objective of EC4MACS is to add the urban dimension in GAINS with the CHIMERE model.

An in-depth analysis of the AIRBASE[3] data recorded in 2009, has been realised to establish simple relationships between yearly averages and the number of exceedances of the threshold values. The following conclusions can be drawn:

- For NO2: if the yearly concentrations remain under the yearly threshold value (40 µg/m^3), the hourly exceedance standards will also be respected.
- For PM10: a linear relationship comes out between the number of daily exceedances of the regulatory threshold value (50 µg/m^3) and the annual mean concentrations (Figure 2).

[3] AirBase is a public air quality database containing air quality monitoring information for more than 30 participating countries throughout Europe (http://www.eea.europa.eu/themes/air/airbase)

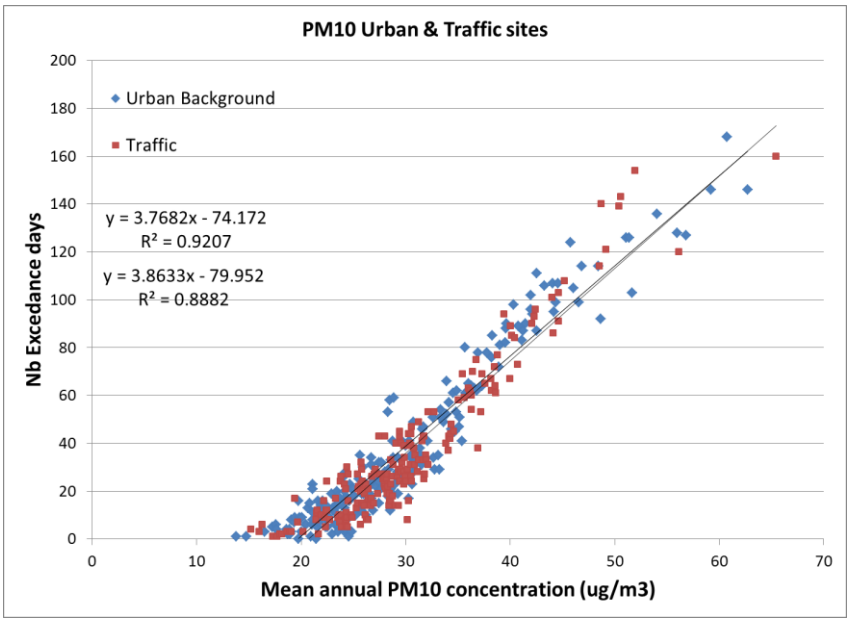

Figure 2 : Relation between the number of daily exceedances and the annual mean concentrations according 2009 AIRBASE data

The previous analysis suggests that the downscaling methodology can be defined on an annual basis for both PM10 and NO2 concentrations. It is noteworthy that for PM10, **if the annual concentrations remain below 27-30 µg/m^3, the yearly and daily standards are both respected.** The CHIMERE model is able to provide an added value at the urban level but cannot reproduce road traffic concentrations. An additional methodology is required to treat these hotspots particularly important for NO2 exceedances.

In this report, the CHIMERE model that has been used to generate a high resolution simulation over a large part of Europe for 2009 is presented. A short model evaluation is proposed in this report. These model outputs will be processed in a follow-up step to obtain a suitable downscaling methodology for the GAINS calculations.

2 Description of CHIMERE

2.1 Short description of CHIMERE in the EC4MACS context

CHIMERE is designed to calculate the concentrations of usual chemical species that are involved in the physic-chemistry of the low troposphere. CHIMERE has been described in detail several times: Schmidt et al. (2001) for the dynamics and the gas phase module; Bessagnet et al. (2004, 2008, 2009) for the aerosol module. The aerosol model species are sulphates, nitrates, ammonium, secondary organic aerosol (SOA), sea-salt and dust. The particles size distribution ranges

from 40 nm to 10 µm and are distributed into 8 bins (0.039, 0.078, 0.156, 0.312, 0.625, 1.25, 2.5, 5, 10 µm). For more detail on the latest development one can refer to the online documentation (http://www.lmd.polytechnique.fr/chimere).

For this study, we defined a nested fine resolution domain named EC4MB (324x410 points) that covered the whole of Europe from 10.4375°W to 29.9375°E in longitude and 35.9062°N to 61.4687°N in latitude with a **resolution of about 7 – 8km**. This resolution is a compromise between computing time capacities and ability to address the urban dimension of the major European cities. A coarse domain encompassing this nested domain has been defined with **a 50 km resolution**. Boundary conditions are monthly mean climatologies taken from the LMDz-INCA (Schulz et al. 2006) model for gaseous species and from the GOCART model (Ginoux et al., 2001) for aerosols (desert dust, carbonaceous species and sulphate). Within EC4MACS, the vertical resolution has been improved close to the ground level. Nine vertical levels are selected with a **first layer height raising at 20-25 m**.

Emissions were issued from the EMEP 0.5x0.5 database[4] for VOC, SOx, NH3, SOx, CO and PM. Six biogenic species (isoprene, α-pinene, β-pinene, limonene, ocimene, and NO) were calculated using the MEGAN model (Guenther et al., 2006). We also accounted for fire emissions from GFED. The fire emissions GFED (Global Fire Emissions Database) are derived from satellite observations (Giglio et al., 2010). These emission data are monthly climatologies available on the 1996-2009 period at 0.5 ° resolution over Europe. Only fire emissions of CO, NOx, SO2 and PM components have been considered in CHIMERE.

After adjusting the methodology with data from the year 2006, the **year 2009** has been selected for the operational calculations in EC4MACS, therefore, CHIMERE has been run over the entire year 2009.

Main missing processes in the EC4MACS CHIMERE simulation

- The resuspension of dust issued from local erosion was not taken into account in this simulation. The current parameterization in CHIMERE (Vautard et al., 2005) for wind blown dust was not activated because the formula strongly depends on wind speed and soil moisture. This latter variable is very difficult to simulate and really dependent on the meteorological driver. This phenomenon affects the PM10 background concentrations only.
- The road dust resuspension process is not implemented in CHIMERE. This process affects PM10 concentrations at the urban level.

[4] http://www.ceip.at/emission-data-webdab/

- The chemistry of semi-volatile organic compounds is not taken into account in CHIMERE. This chemistry mainly affects the share ratio of primary versus secondary organic species over urban areas. The total mass of organic aerosols is less affected. Nevertheless, the theory behind suggests a missing mass of semi-volatile species that is not reported in emission inventories.
- The formation of coarse nitrate (nitrate in the coarse mode of particles) is not implemented in CHIMERE.

2.2 Gas phase chemistry

The set of chemical reactions follows the work of Lattuati (1997) (a modified version of the mechanism proposed by Hov et al. (1985) with updated reaction rates. Clear-sky photolysis rates are now tabulated from the Tropospheric Ultraviolet and Visible model (TUV, Madronich and Flocke, 1998) and depend on altitude. As described by Schmidt et al. (2001), the model columns are assumed to lie ‘‘below the clouds’’ since cloud effects on photolysis rates are taken into account using a single attenuation coefficient throughout a model column. All photolysis rates are modulated as :

$$J = J_c(\zeta, z)\exp\left(-aD^{2/3}\right)$$

where $J_c(\zeta, z)$ is the clear-sky photolysis rate, depending on zenith angle ζ and altitude z; D is the cloud optical depth and a=0.11 is an adjusted coefficient obtained by regression from several TUV calculations with various cloud hypotheses.

2.3 Aerosols

Atmospheric aerosols are represented by their size distributions and compositions. The sectional representation described by Gelbard and Seinfeld (1980) has been used for the density distribution function. The sectional approach is quite useful to solve the governing equation for multicomponent aerosols. It discretizes the density distribution in a finite number of bins (Warren, 1986). Thus, all particles in section *l* have the same composition and are characterized by their mean diameter d_l. The aerosol module actually uses 8 bins from 40nm to 10 µm, following a geometrical progression. For a given *x* as x=ln(m); with m the particle mass, q(x) is the density distribution defined by $q(x) = \frac{dQ}{dx}$, Q being the mass concentration function.

Q_l^k (µg/m^3) is the mass concentration of component k in section l and Q_l (µg/m^3) is the total mass concentration in section l.

$$Q_l = \int_{x_{l-1}}^{x_l} q(x)dx = \sum_k Q_l^k$$

In the model, particles are composed of species listed in Table 2. Sulfate is formed through gaseous and aqueous oxidation of SO2. Nitric acid is produced in the gas phase by NOx oxidation. N_2O_5 is converted into nitric acid via heterogeneous pathways by oxidation on aqueous aerosols. Ammonia is a primary emitted base converted in the aerosol phase by neutralization with nitric and sulfuric acids. Ammonia, nitrate and sulphate exist in aqueous, gaseous and particulate phases in the model. As an example, in the particulate phase the model species pNH3 represents an equivalent ammonium as the sum of NH4 ion, NH3 liquid, NH4NO3 solid, etc. For semi-volatile inorganic species (sulfate, nitrate, ammonium), the equilibrium concentration is calculated using the thermodynamic module ISORROPIA (Nenes et al., 1998). This model also determines the water content of particles. The partitioning process is fully described in Bessagnet et al. (2004). The secondary organic aerosols (SOA) are described in the next subsection.

Table 2 : List of aerosol species in CHIMERE (with model name and type). SOA are split in several species described in the next section

Species	**Expanded name**	**Origin**
PPM	Anthropogenic primary species (EC, OC and other primary compounds)	Primary
SOA	Secondary Organic Aerosols	Secondary
DUST	Desert dust (from the boundaries)	Primary
H2SO4	Sulphate	Secondary
NO3	Nitrate	Secondary
NH4	Ammonium	Primary emitted and transferred in particles
WATER	Water (excluded in the PM10 outputs)	Transferred in particles

2.4 Secondary organic chemistry

A specific SOA (Secondary Organic Aerosols) module has been used for this study, the complete chemical scheme implemented in CHIMERE includes biogenic and anthropogenic precursors (Table 3). Biogenic precursors include API (α-pinene and sabinene), BPI (β- pinene and δ^3-carene), LIM (limonene), TPO

(myrcene and ocimene) and ISO (isoprene). Anthropogenic precursors include TOL (benzene, toluene and other mono-substituted aromatics), TMB (Trimethylbenzene and other poly-substituted aromatics), and NC4H10 (higher alkanes). SOA formation is represented according to a single-step oxidation of the relevant precursors and gas-particle partitioning of the condensable oxidation products. The overall approach consists in differentiating between hydrophilic SOA that are most likely to dissolve into aqueous inorganic particles and hydrophobic SOA that are most likely to absorb into organic particles. The dissolution of hydrophilic SOA is governed by Henry's law whereas the absorption of hydrophobic particles is governed by Raoult's law. The large number of condensable organic compounds is represented by a set of surrogate compounds that cover the range of physico-chemical properties relevant for aerosol formation, i.e., water solubility and acid dissociation for hydrophilic compounds and saturation vapour pressure for hydrophobic compounds. These surrogate compounds were selected by grouping identified particulate-phase molecular products with similar properties. The molecular weight of each surrogate compound is determined based on its structure and functional groups. The Henry's law constant or the saturation vapour pressure of the surrogate species is derived from the average properties of the group. Other properties are estimated using the structure of each surrogate compound. Enthalpy of vaporization are given in brackets (kJ/mol) for each SOA compounds: AnA0D (88), AnA1D(88), AnA2D(88), BiA0D(88), BiA1D(88), BiA2D(109), AnBmP(88), AnBlP(88), BiBmP(175).

Table 3 : Gas phase chemical scheme for SOA formation in CHIMERE

Reactions	Kinetic rates (*molecules cm*$^{-3}$ *s*$^{-1}$)
TOL+OH → 0.004×AnA0D + 0.001×AnA1D + 0.084×AnBmP + 0.013×AnBlP	$1.81\times10^{-12}\exp(355/T)$
TMB+OH → 0.002×AnA0D + 0.002× AnA1D + 0.001×AnA2D + 0.088×AnBmP + 0.006×AnBlP	$9.80\times10^{-9}/T$
NC4H10+OH → 0.07×AnBmP	$1.36\times10^{-12}\exp(190/T)^{-2}$
API+OH → 0.30×BiA0D + 0.17×BiA1D + 0.10×BiA2D	$1.21\times10^{-11}\exp(444/T)$
API+O3 → 0.18×BiA0D + 0.16×BiA1D + 0.05×BiA2D	$1.01\times10^{-15}\exp(-732/T)$
API+NO3 → 0.80×BiBmP	$1.19\times10^{-12}\exp(490/T)$
BPI+OH → 0.07×BiA0D + 0.08×BiA1D + 0.06×BiA2D	$2.38\times10^{-11}\exp(357/T)$
BPI+O3 → 0.09×BiA0D + 0.13×BiA1D + 0.04×BiA2D	1.50×10^{-17}
BPI+NO3 → 0.80×BiBmP	2.51×10^{-12}
LIM+OH → 0.20×BiA0D + 0.25×BiA1D + 0.005×BiA2D	1.71×10^{-10}
LIM+O3 → 0.09×BiA0D + 0.10×BiA1D	2×10^{-16}
TPO+OH → 0.70×BiA0D + 0.075×BiA1D	$5.10\times^{-8}/T$
TPO+O3 → 0.50×BiA0D + 0.055×BiA1D	$7.50\times10^{-14}/T$
TPO+NO3 → 0.70×BiA0D + 0.075×BiA1D	$4.30\times10^{-9}/T$
ISO+OH → 0.232×ISOPA1 + 0.0288×ISOPA2	$2.55\times10^{-11}\exp(410/T)$

The surrogate SOA compounds consist of six hydrophilic species that include an anthropogenic non-dissociative species (AnA0D), an anthropogenic once-dissociative species (AnA1D), an anthropogenic twice-dissociative species (AnA2D), a biogenic non-dissociative species (BiA0D), a biogenic once-dissociative species (BiA1D) and a biogenic twice-dissociative species (BiA2D), three hydrophobic species that include an anthropogenic species with moderate saturation vapor pressure (AnBmP), an anthropogenic species with low saturation vapor pressure (AnBlP) and a biogenic species with moderate saturation vapor pressure (BiBmP), and two surrogate compounds for the isoprene oxidation products (ISOPA1, ISOPA2). T is the temperature in K.

The full name of compounds is given in Table 3 caption. The absorption process in CHIMERE is implemented as in Bowman et al. (1997). A dynamical approach is adopted to describe the gas/particle conversion since the model time-step is about 5 min and using the approach described in Bowman et al. (1997), the characteristic time for mass transfer can exceed 20 min for coarse particles.

$$J_i = \frac{1}{\tau_i}\left(G_i - G_i^{eq}\right)$$

J_i (µg/m^2/s) is the absorption or desorption flux of species i, τ_i (s) is a characteristic time of the mass transfer that depends on particle size and the chemical properties of species i, G_i is the bulk gas-phase concentration of species i and G^{eq} is the gas phase concentration of species i at thermodynamic equilibrium (i.e., at the surface of the particle). The equilibrium gas-phase concentrations are functions of the particle chemical composition, temperature and, for hydrophilic species, relative humidity, as described in Pun et al. (2006).

The base SOA module was tested against smog chamber data (Odum et al. 1997) for anthropogenic compounds and for biogenic compounds (Griffin et al. 1999) and was shown to satisfactorily reproduce SOA formation for those compounds (Pun et al. 2006). In this study, higher alkanes and isoprene were added to the original

chemical mechanism. The formation of SOA from higher alkanes follows the formulation used in Zhang et al. (2007) for the stoichiometric SOA yield and it is assumed that the SOA species can be represented by a hydrophobic surrogate compound with a moderate saturation vapour pressure. The formation of SOA from the oxidation of isoprene by hydroxyl radicals is represented with two surrogate products and follows the formulation prescribed in Kroll et al. (2006); Zhang et al. (2007).

2.5 Landuse data in CHIMERE

CHIMERE requires land use data at high resolution at different stages in the model (Table 4).

Table 4 : Type of land use databases used for different processes in CHIMERE

Process	**Landuse name**
Biogenic emission calculations	GLOBCOVER
Deposition calculations	GLOBCOVER
Anthopogenic emission regridding	USGS
Correction of meteorology	GLOBCOVER

USGS[5] Land use database

This 24 categories land use databse is provided at 1km resolution over the world. These data are those implemented in the mesoscale meteorological model WRF[6].

GLOBCOVER Land use database

The GlobCover Land Cover is a global land cover map at 10 arc second (300 meter) resolution (Bicheron et al., 2008). It contains 22 global land cover classes defined within the UN Land Cover Classification System (LCCS). GlobCover database is based on the ENVISAT satellite mission's MERIS sensor (Medium Resolution Image Spectrometer) Level 1B data acquired in Full Resolution (FR) mode with a 300 meters spatial resolution. GlobCover LC was derived from an automatic and regionally-tuned classification of a time series of MERIS FR composites covering the period December 2004-June 2006.

[5] US Geological survey (http://www.usgs.gov/)

[6] The Weather Research and Forecasting (WRF) Model is a next-generation mesoscale numerical weather prediction system designed to serve both operational forecasting and atmospheric research needs. It features multiple dynamical cores, a 3-dimensional variational (3DVAR) data assimilation system, and a software architecture allowing for computational parallelism and system extensibility. WRF is suitable for a broad spectrum of applications across scales ranging from meters to thousands of kilometres (http://www.wrf-model.org).

For both land use databases, the “water bodies” class was broken down in two categories thanks to a Land/Sea mask at 1km resolution :

- Ocean & seas
- In land waters

3 Meteorology

3.1 Input data

CHIMERE is an off-line chemistry-transport model driven by meteorological fields, e.g., from a weather forecast model, such as WRF or directly from meteorological reanalyses. CHIMERE contains a meteorological pre-processor that prepares standard meteorological variables to be read by the model core (

Table 5).

Table 5 : List of meteorological variables required by CHIMERE in the pre-processing stage

File Name	Variable	Dimension	Units
Mandatory Variables			
lon	longitude of gridpoints	2D	degrees_east
lat	latitude of gridpoints	2D	degrees_north
winz	Zonal component of the wind	3D	m/s
winm	Meridional component of the wind	3D	m/s
temp	Temperature	3D	K
sphu	Specific humidity	3D	kg/kg
alti	Altitude of half layers on which all 3D meteo variables should be given	3D	m
pres	Pressure at half layers on which all 3D meteo variables should be given	3D	Pa
cliq	3D cloud liquid water content for radiation (excluding rain water)[1]	3D	Kg/Kg
tem2	2m Temperature	2D	K
copc	Convective Precipitation[1]	2D	kg/m^2/hour
lspc	Large-scale Precipitation[1]	2D	kg/m^2/hour
Optional Variables			
rain	3D rain water (to be added to cloud water for radiation)	3D	Kg/Kg
cice	3D ice (for radiation)	3D	Kg/Kg
sshf	Surface sensible heat flux, optionally read or recalculated	2D	W/m2
slhf	Surface latent heat flux, optionally read	2D	W/m2
flux	Virtual heat flux, optionally read or recalculated from Priestley (1948)	2D	W/m2
psfc	Surface pressure, optionally read	2D	Pa
usta	Friction velocity, optionally read or recalculated from Louis [1982]	2D	m/s
hght	Boundary layer height, optionally read or recalculated	2D	m
lowc	Low cloud fraction, optional for radiation	2D	m
medc	Medium cloud fraction, optional for radiation	2D	m
higc	High cloud fraction, optional for radiation	2D	m

3.2 Horizontal transport

Three schemes for horizontal transport of chemical concentrations in the model are now available. The schemes are:

- A simple first-order upwind scheme named upwind in the model: low computational cost but not very accurate and very diffusive.
- The second-order Van Leer scheme: low computational cost and good accuracy for transport of high concentrations in plumes.
- The third-order PPM scheme (PPM stands for 'Parabolic Piecewise Method'), proposed by Colella and Woodward (1984): high computational cost but more accurate for long-live species, naturally diffusive in a chemistry-transport model

For the EC4MACS project we selected the PPM scheme

3.3 Turbulent mixing in CHIMERE

Horizontal turbulent fluxes are not considered. Vertical turbulent mixing takes place only in the boundary layer. The formulation uses K-diffusion following the parameterization of Troen and Mahrt (1986), without counter-gradient term. In each model column, diffusivity K(z) is calculated as:

$$K(z) = k w_s z \left(1 - \frac{z}{h}\right)^{1/3}$$

where w_s is a vertical scale given by similarity formulae.

- In the stable case (surface sensible heat flux < 0): $w_s = u_*/(1 + 4.7\, z/L)$
- in the unstable case : $w_s = ({u_*}^3 + 2.8 e {w_*}^3)^{1/3}$

where e = *max(0.1,z/h)*, L is the Obukhov Length, w_* is the convective velocity scale, u_* the friction velocity and h the boundary layer height. A minimal K(z) is assumed, with a value of 0.01 m^2/s.

The boundary layer height h can be either directly provided by the meteorological model or recalculated in the CHIMERE preprocessing. In the latter case the boundary layer height is considered as the maximum of the Troen and Mahrt (1986) boundary layer height calculated from the Richardson number profile, as the lowest altitude where $R_i = 0.5$, and a more convectively-based boundary layer height calculation. The latter is based on a simplified and diagnostic version of the approach of Cheinet (2002). It consists in the resolution of the (dry) thermal plume equation with diffusion. The in-plume vertical velocity and buoyancy equations are solved and the boundary layer is taken as the height where vertical velocity stops. Thermals are initiated with a non-vanishing vertical velocity and potential temperature departure, depending on the turbulence similarity parameters in the surface layer.

At each interface between layers k and k+1, one calculates an equivalent turbulent vertical velocity V_k and vertical mixing is expressed in layer k by the mass flux:

$$Flux = \frac{V_k}{H_k}\left(C_{k+1}\frac{D_k}{D_{k+1}} - C_k\right)$$

where *C* denotes concentrations, *D* air densities and *H* layer thicknesses. Density ratios are applied since turbulent mixing must conserve mass in each model cell. An equivalent formula is used for the upper layer. The turbulent velocity V_k is deduced from K(z) using:

$$V_k = \frac{Kz}{\frac{1}{2}(H_k + H_{k+1})}$$

3.4 Selected meteorology and urban corrections

As CHIMERE is an off-line model, we had to select a set of meteorological data that was available for the entire 2009 year. For this study, we moved from the usual WRF limited area models to the ECMWF Integrated Forecast System (IFS) data (http://www.ecmwf.int/research/ifsdocs). Motivations included the systematic over estimation of wind speed by WRF (Jimenez and Dudhia, 2012) and the save in time allowed when using directly IFS data because the intermediate step to get meteorological pre-runs is removed. These differences have been confirmed by the calculation of statistics on wind speeds at regional stations (Figure 3). A deeper study shows that WRF enhances the wind speeds up to 20% in particular configurations.

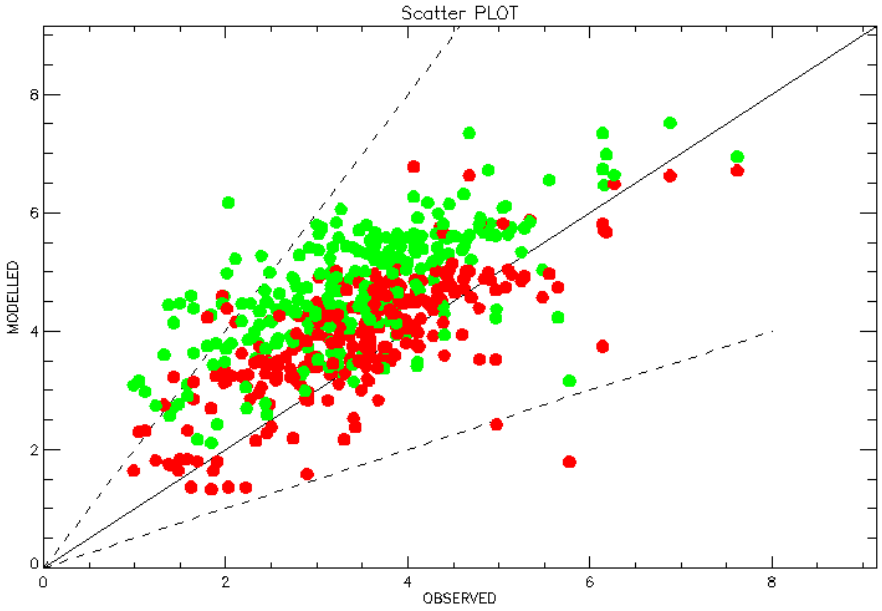

Figure 3 : Wind speeds (m/s) between IFS (red circles) and GFS/WRF (green circles) – Observed versus modelled values

The IFS model has a 0.25x0.25° horizontal grid spacing from surface to 0.1 hPa (91 levels). It delivers typical meteorological variables (temperature, wind components, specific humidity, pressure, sensible and latent heat fluxes) that are vertically and horizontally interpolated onto the CHIMERE grid (9 levels).

Nevertheless, the problem remains over urban areas. Indeed, IFS provides meteorological variables representative of the regional scale. Urban local effects are not taken into account in the IFS reanalysis. Most of the air pollutant observations are available in the urban sublayer and the urban canopy and the objective is to calculate pollutant concentrations in those layers.

Unfortunately, meteorological models or reanalysis at such horizontal resolution (20km) cannot reproduce the urban meteorology in the urban canopy and urban

sublayer over such a large domain (the whole Europe). This has an impact on the vertical diffusion of primary pollutant concentrations (O3, NO2 and PM) and their transport close to the ground within the city (Figure 4).

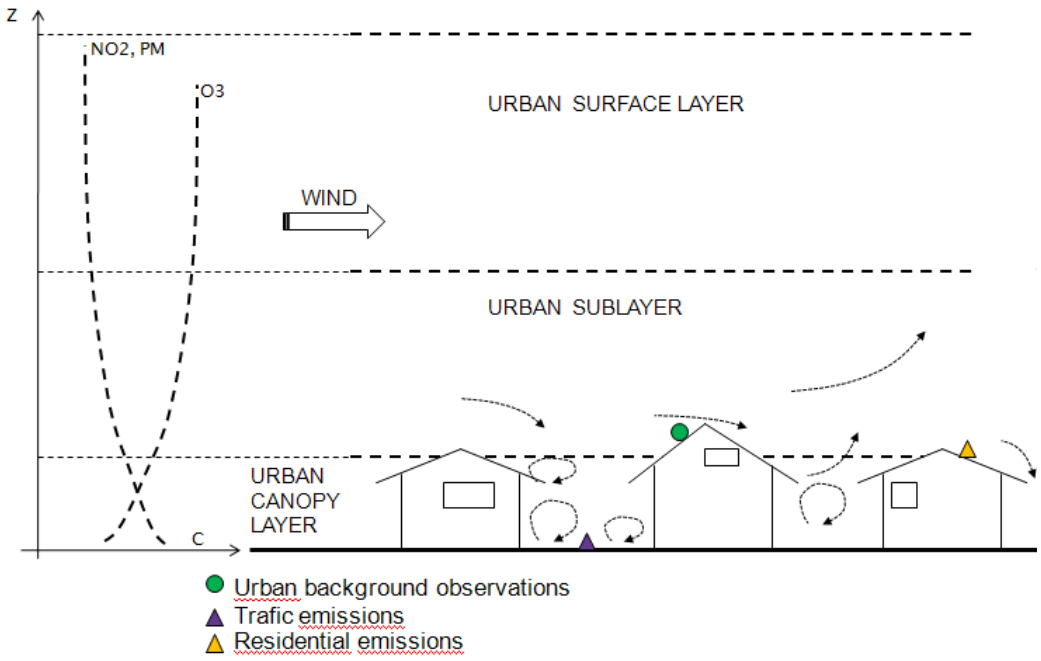

Figure 4 : Influence of meteorology at the urban level. O3 concentrations will be lower at the ground level titration and deposition effect) whereas NO2 and PM concentrations will be higher (vicinity of emissions).

To account for the urban effect on meteorology, **the wind speed and the vertical diffusion (Kz) were modified** in the EC4MACS version of CHIMERE.

- ***Wind speed***

Usually, operational meteorological observations are performed far from urban areas for representativeness reasons. Some study reveals large differences between urban and rural winds (Fisher et al. 2005, Siedlecki) showing wind speed ratio (urban –rural) up to 0.5.

Within the modelling case of Lisbon (Solazzo et al., 2010), the ratio between wind speed inside the canopy and at the top of the urban sublayer was in the range 0.1 and 0.6.

For those reasons we decided do arbitrary multiply the wind speed by 0.5 computed in the first CHIMERE level.

- ***Vertical diffusion (Kz)***

In dispersion models at the urban scale, the lower part of the boundary layer is often represented using parameterizations derived from the theory of similarity of the surface layer. The urban effects are then considered by changes in surface roughness and heat flux. Nevertheless, these formulations should only be used in the inertial sublayer (ISL) which is well above the tops of the building.

Indeed, in the sub-rough layer (RSL or urban sublayer), *i.e*. in the immediate vicinity of the urban canopy elements, the flow has a rather complex structure (Raupach, 1980) and the similarity theory cannot be applied. Rotach (1993, 1995) analyzed mean flow and turbulence measurements inside and above an urban street canyon. He found that one of the characteristic features of the RSL is an increase in the absolute value of Reynolds stress, from essentially zero at the average zero plane displacement height up to a maximum value, which he observed at about two times the average building height. The RSL extends from the ground to a level where horizontal homogeneity of the flow is well established, so about 2 to 5 times the average height of the elements of the canopy (Raupach et al., 1991) or up to several tens of meters in major cities.

In a first approach, the Schmidt number defined by the ratio of diffusivity of momentum and mass diffusion coefficient is taken equal to 1. Considering this, Kz is given by :

$$Kz = \frac{-\overline{u'w'}}{\frac{\partial u}{\partial z}}$$

Considering this, we can assume at urban ground level a negligible value of Kz. Then Kz should increase with the Reynolds stress to a maximum value at 2 to 5 times the average height of the buildings.

This first level of CHIMERE is currently 20 m. This is clearly two times under the average of the buildings height in big cities. So that we can assume that the corresponding Reynolds stress at this level has not yet reach his maximum value and the corresponding value of Kz is overestimate even if we can also assume that Kz is underestimate at the second level of CHIMERE. At the first level of chimere, Kz should be given by :

$$Kz = \int_{z=0}^{z=1st\ level} \frac{-\overline{u'w'}}{\frac{\partial u}{\partial z}}\, dz$$

In a first approach, if we assume that the theory of similarity is applicable above the first level, we can take for urban areas :

$$Kz\ (z < first\ level) = \frac{Kz\ (first\ level\ computed\ with\ the\ similarity\ theroy)}{2}$$

Therefore, the Kz has been multiplied by 0.5 in the first layer.

These wind speed and Kz corrections are certainly underestimated for the mixing of ground emissions like road traffic emissions. An additional correction factor or a virtual layer to delay the mixing of ground **emissions could also be added in the future CHIMERE developments.**

4 Emissions

4.1 Biogenic emission from soil and vegetation

Emissions of six CHIMERE species: isoprene, α-pinene, β-pinene, limonene, ocimene, and NO, are calculated using the MEGAN model data and parameterizations. The MEGAN model (Guenther et al., 2006), exploits most recent measurements in a gridded and canopy scale approach, more appropriate for use in CTMs since it estimates the effective burden of gases that mix and react in the boundary layer. Estimates of biogenic VOCs from vegetation and NO emissions are calculated as :

$$ER_i = EF_i \times \gamma_i(T, PPFD, LAI) \times \rho_i$$

where ER_i (µg/m^2/h) is the emission rate of species i, EF_i µg/m^2/h) is an emission factor at canopy standard conditions, γ_i (unitless) is an emission activity factor that accounts for deviations from canopy standard conditions, and ρ_i is a factor that accounts for production/loss within canopy. The canopy standard conditions relevant for this study are defined as: air temperature (T) of 303 K, photosynthetic photon flux density (PPFD) of 1500 µmol/m^2/s at the top of the canopy, leaf area index (LAI) of 5 m^2/m^2 and a canopy with 80% mature, 10% growing and 10% old foliage. The MEGAN model parameterizes the bulk effect of changing environmental conditions using three time-dependent input variables specified at top of the canopy: temperature (T), radiation (PPFD), and foliage density (LAI). The production/loss term within canopy is assumed to be unity (ρ=1).

The MEGAN model provides input EF and LAI data over a global grid, herefater projected on the CHIMERE model grid. The current available choice for EFs is restricted to following species: isoprene, α-pinene, β-pinene, myrcene, sabinene, limonene, δ^3-carene, ocimene, and nitrogen oxide. EF's are static and refer to

years 2000-2001. They are obtained summing up over several plant functional types (e.g. broadleaf and needle trees, shrubs, etc...). LAI database is given as a monthly mean product derived from MODIS observations, referred to base year 2000. Hourly emissions are calculated using 2-m temperature and short-wave radiation from a meteorological model output. Terpene and humulene emissions are not calculated in this model version and are set to zero.

4.2 Sea salt emissions

Sea salt emissions are calculated by Monahan (1986) :

$$\frac{dF}{dr} = 1.373 U_{10}^{3.41} r^{-3} (1 + 0.057 r^{1.05}) 10^{1.19 e^{-B^2}}$$

$$B = \frac{0.38 - \log(r)}{0.65}$$

F is the flux of sea salt particle number in *particles/m²/s/µm*, *r* the particle radius in *µm* and U_{10} is the wind speed at 10 m in *m/s*.

4.3 Anthropogenic emissions

The aim of the emission pre-processor is to transform raw anthropogenic emissions (ton/year/country) to CHIMERE compliant emissions (Figure 5). The raw data per activity sector comes from annual inventories. VOC, NOx, CO, SO_2, NH_3, PPM (primary particle material) annual emissions come from the Co-operative Programme for Monitoring and Evaluation of the Long-range Transmission of Air pollutant – EMEP – (Vestreng, 2003).

Annual NOx emissions are speciated using ratio NO/NO2 ratio recommended by IIASA (personal communication). For NMVOC, a speciation is obtained over 32 NMVOC NAPAP classes (Middleton et al., 1990). Time disaggregation is done on the basis of EMEP data using monthly, weekly and hourly coefficients depending on the activity sector. In a second time, an aggregation step is performed for the lumping of NMVOCs into model species following Middleton et al. (1990). Finally, hourly values of surface anthropogenic emissions are available for 15 primary pollutants: NO, NO2, CO, SO_2, CH_4, and the ten following non-methane volatile organic compounds (NMVOC): Ethane, n-butane, ethene, propene, o-xylene, formaldehyde, acetaldehyde, methyl, ethyl-ketone, ethanol and ethanol.

The list of level 1 SNAP sectors are :

1. Combustion in energy and transformation industries
2. Non-industrial combustion plants
3. Combustion in manufacturing industry
4. Production processes
5. Extraction and distribution of fossil fuels and geothermal energy
6. Solvent and other product use
8. Other mobile sources and machinery
9. Waste treatment and disposal
10. Agriculture
11. Other sources and sinks

Five main steps can be identified in the anthropogenic emission pre-processing: (1) the spatial regridding of the raw emission to comply with the CHIMERE grid, (2) the temporal disaggregation, (3) the chemical speciation, (4) the hourly disaggregation and (5) the surface flux calculation within CHIMERE (Menut et al., 2012).

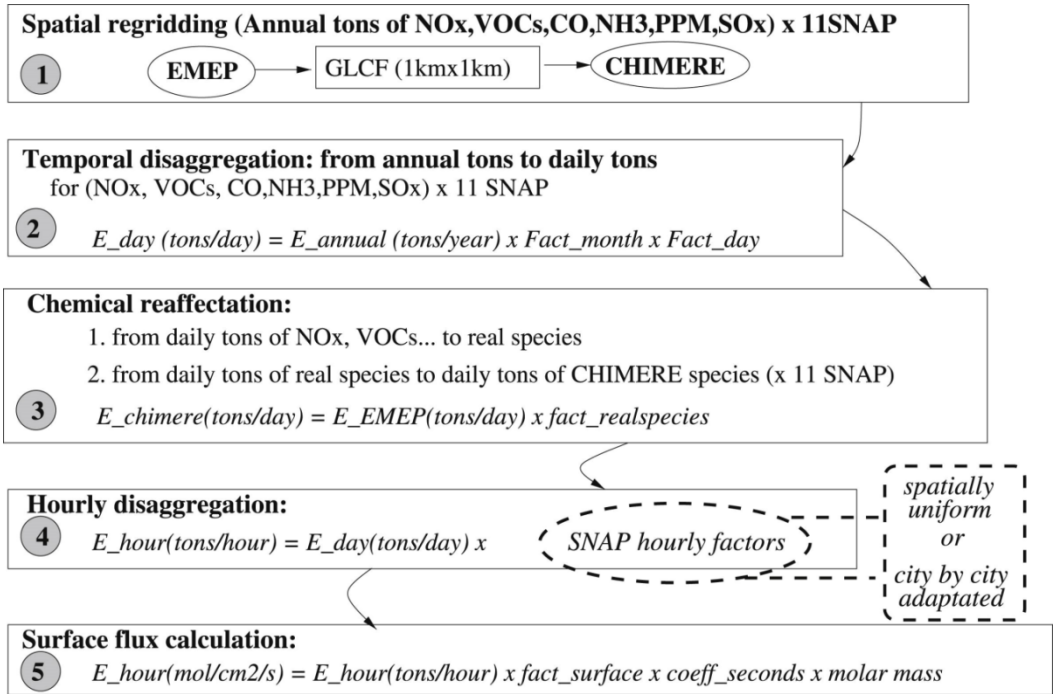

Figure 5 : The EMEP to CHIMERE emission converter

The first step in CHIMERE consists in regridding the anthropogenic emission inventory EMEP at 0.5°x0.5° resolution onto the CHIMERE computational grid using the USGS database. Its high resolution (1km) preserves accuracy on emission spatialisation. Twenty-eight landuse categories exist in the USGS database. Only “crops”, “grasslands”, “urbanized area” and “forest” categories are used to downscale the emissions.

For EC4MACS, the emission pre-processor has been modified to allow emissions from SNAP2 to be disaggregated according to the population density (Figure 7). The goal of this approach is to better capture the horizontal variability of the SNAP2 emissions sector. The population data are provided by the JRC[7] over a regular grid at 0.083x0.083° resolution. For the elaboration SNAP2 emissions, we also make a distinction between gaseous and PM species to better reallocate the biomass burning emissions from this sector over the rural areas. Indeed, according to the French bottom-up data issued from the national emission inventory, there is clear evidence that PM2.5 emissions per inhabitant sharply decrease with the population density (Figure 6). This is due to the large contribution of wood burning in individual heating systems that emits large amounts of PM (use of fireplaces).

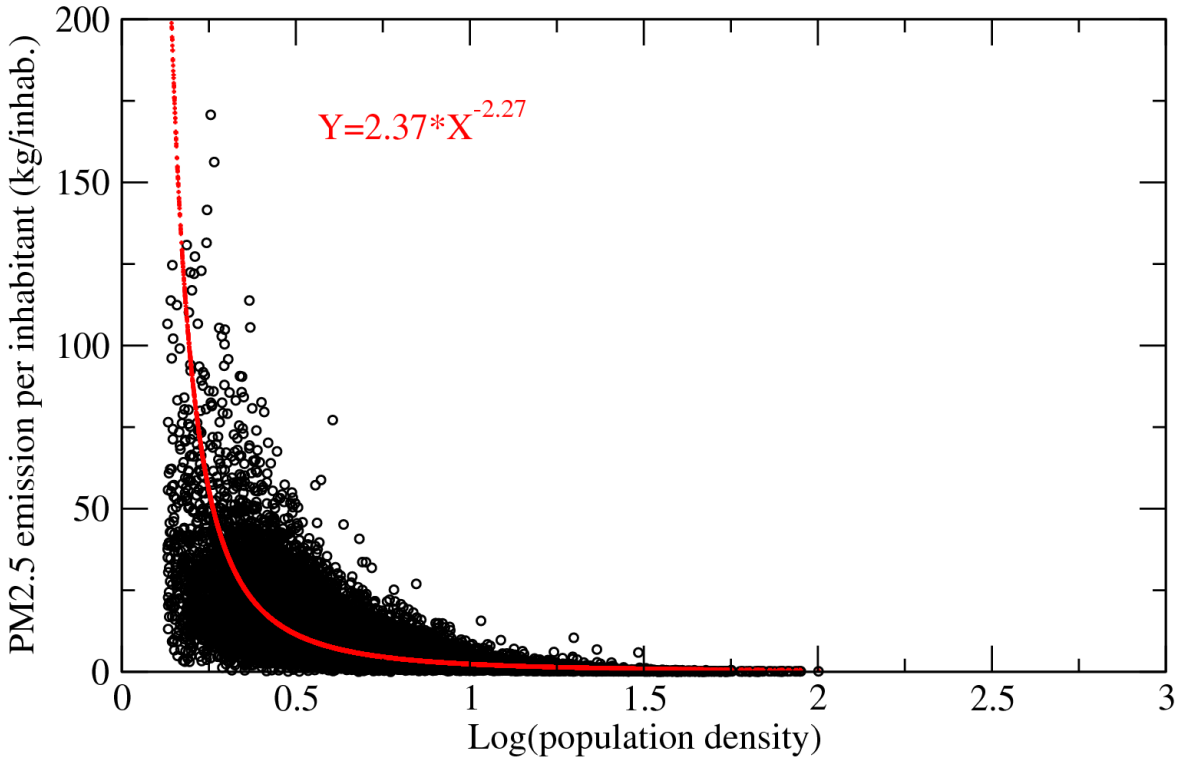

Figure 6 : Evolution of PM2.5 residential emissions per inhabitant (kg/inh/year) as a function of population density (source : French National Emission Inventory). The red curve is the corresponding logarithmic regression used in the CHIMERE emission pre-processor.

[7] Joint Research Centre

Finally, total emissions used in CHIMERE are computed by simply averaging the emission fluxes from each landuse/population cell belonging to its "mother" CHIMERE cell. For SNAP2, we also use a new temporal modulation of SNAP2 emissions according to 2m temperature. The underlying idea is to modulate residential emissions (SNAP2) according to the daily "degree days" concept. The degree day is an indicator used as a proxy variable to express the daily energy demand for heating. The degree day for a day *j* is defined as:

D_j = max(0, 20-T_D) where T_D is the daily mean 2m air temperature. Daily modulation factor (F_j) is therefore defined as: $F_j = D'_j / \overline{D'}$. Where $D'_j = D_j + A.\overline{D}$ and $\overline{D'} = (1 + A).\overline{D}$ where *A* is a user defined modulation factor account for other kind of emissions (e.g. production of hot tap water). $\overline{D}$ is the yearly mean "degree day". The factor F_j is applied to each hourly emission flux.

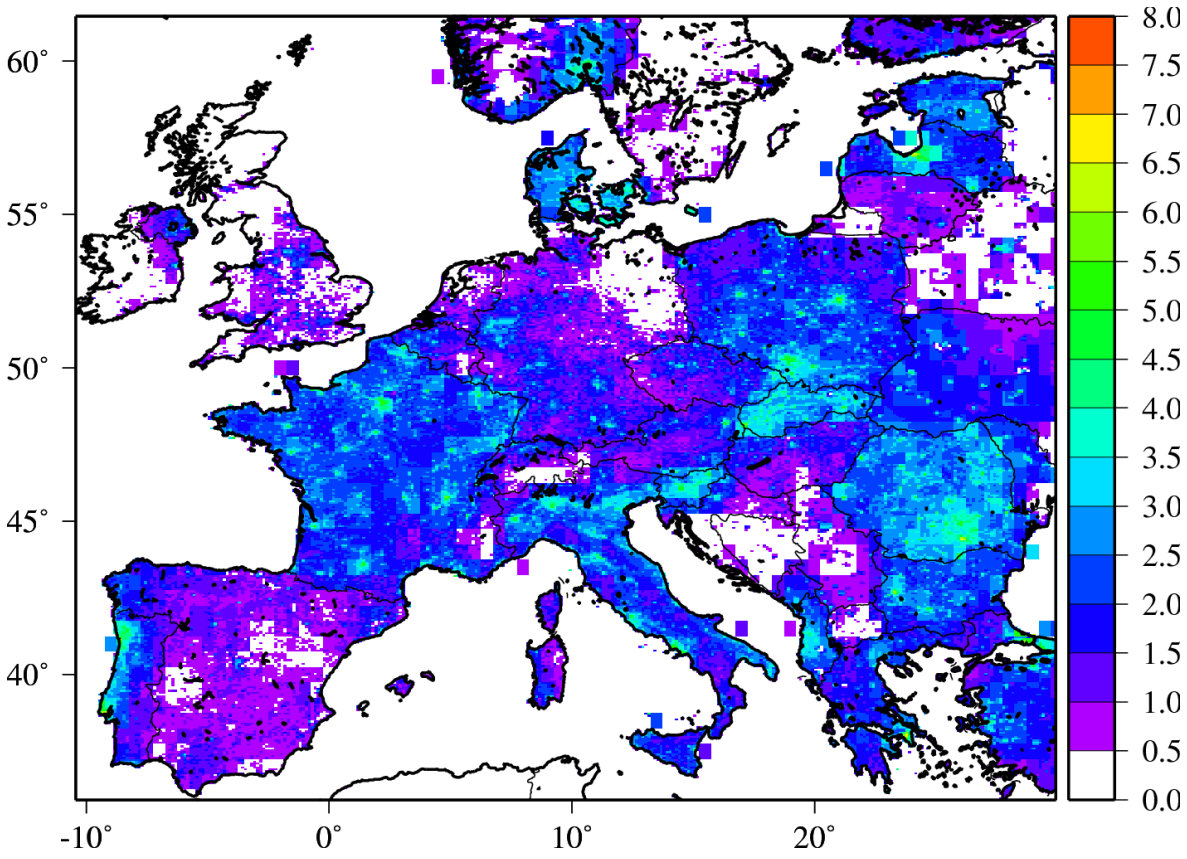

Figure 7 : Primary PM2.5 emissions (SNAP2) regridding using the population density proxy in 2009 (Log(Emission)).

5 Results

5.1 Observational data

Pollutant observations come from two different databases. The first one is the Airbase database (http://acm.eionet.europa.eu/databases). For this study we use two different Airbase types of station: the Rural Background stations (RB) and Urban Background stations (UB). The second database comes from the EMEP network (http://www.emep.int/) that provides pollutants measures concentrations at remote Rural Background sites (RB). The stations are selected if 75% or more data are available over the year. Figure 8 displays the spatial distribution of the AIRBASE (green for RB and blue for UB) and the EMEP (red) stations used for the evaluation. We observe than the spatial repartition is homogenous over the populated regions of Europe but gaps are noted in eastern European and in Balkans countries. The AIRBASE network provides observations for PM10, PM2.5, NO2 and O3. In total, it includes far more stations (RB = 560, UB = 1009) than the EMEP one (RB = 85) and therefore it will prevail in the model evaluation. Details about the stations type of classification and the different measurements techniques are available through the Airbase and EMEP previously quoted websites. We performed the model evaluation using the comprehensive Atmospheric Model Evaluation Tool software (AMET) to calculate three key statistical indexes in order to perform diagnostic evaluation of the model: the correlation index (R), the root mean square error (RMSE) and the fractional bias (FB). Details about the calculation of the statistics using AMET can be found in Appel et al. (2011). The following section is based on yearly and seasonal mean statistics.

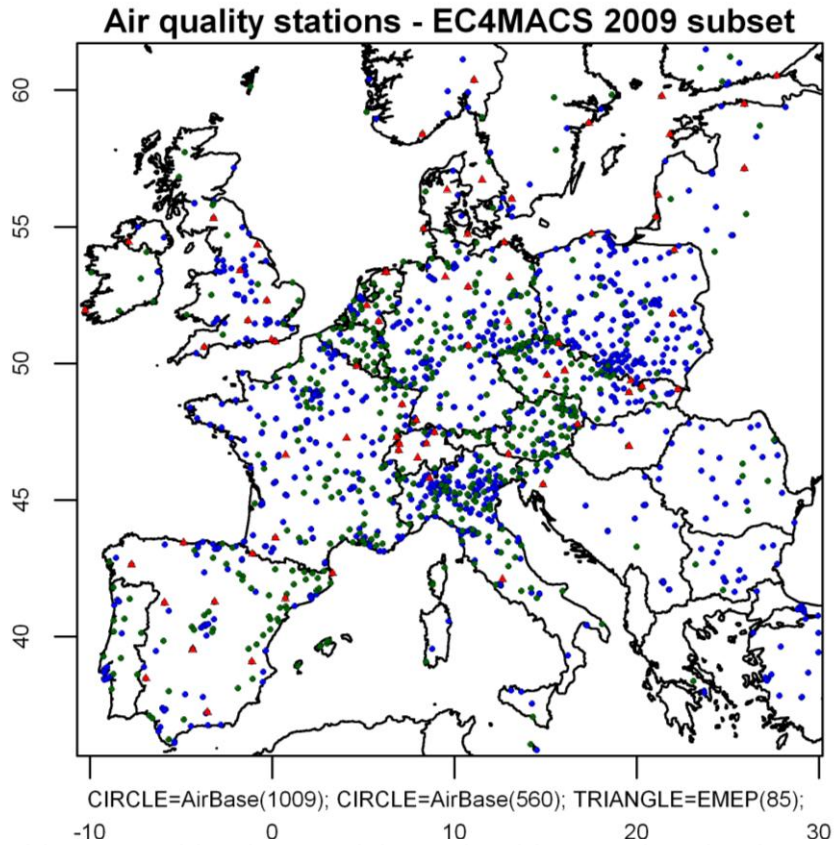

Figure 8 : Airbase rural background (green), Airbase urban background (blue) and EMEP rural background stations (red) projected on the EC4MACS domain used for the evaluation.

5.2 Evaluation with statistic indicators

Figure 9 shows daily box-whisker plots time series of the NO2, O3, PM10 and PM2.5 observed and calculated concentration averaged over all UB Airbase stations.

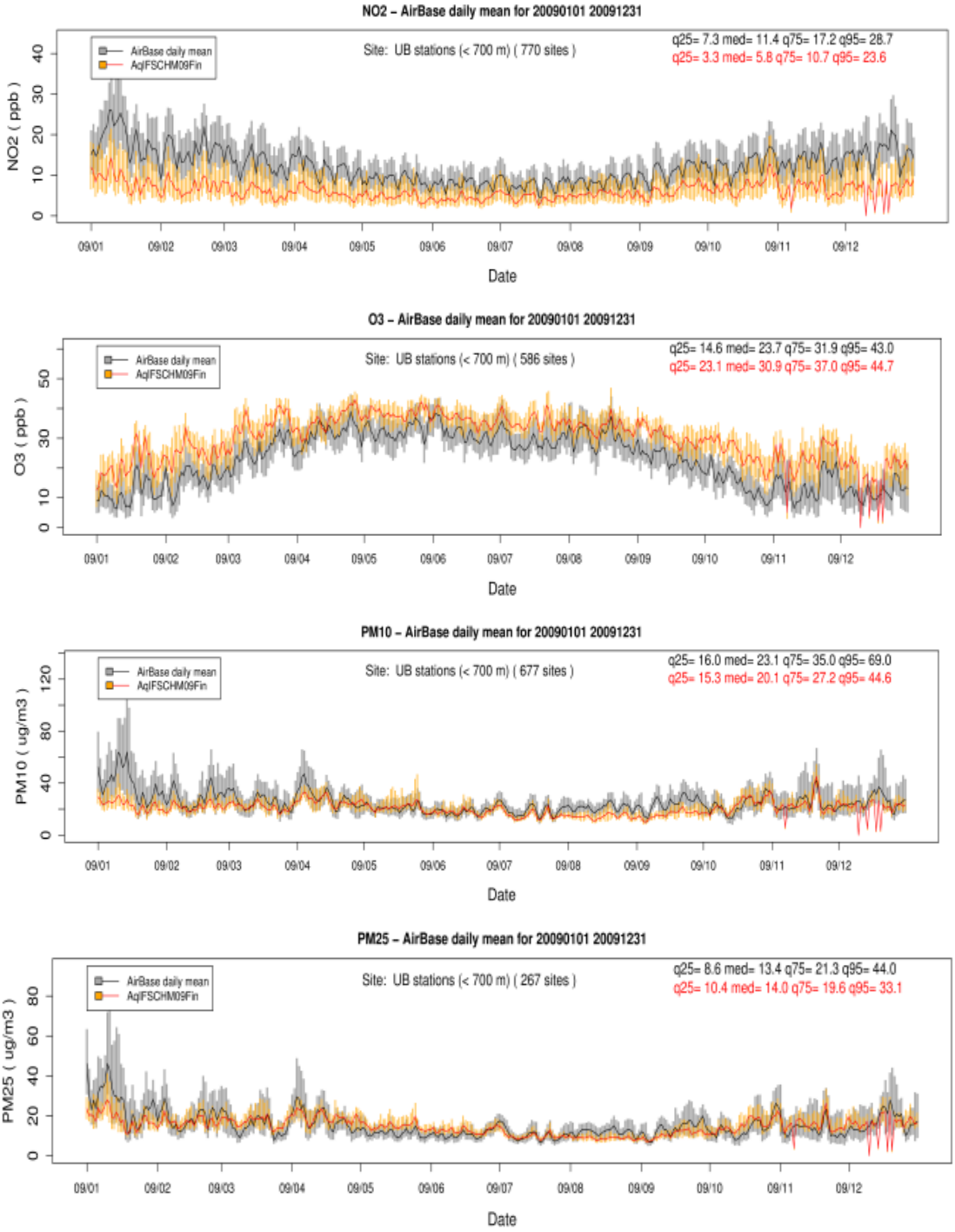

Figure 9 : Daily box-whisker plots time series of the NO2, O3, PM10 and PM2.5 observed and calculated concentration averaged over all UB Airbase stations. The continuous lines represent the medians and the bars show the 25th -75th quantile interval. The yearly 25th, 50th, 75th, and 95th quantiles are reported on the top right corner of the plots.

Table 6 presents a few yearly mean statistical indexes for gas and particulate pollutants. Along the year, CHIMERE captures nicely the temporal variability of NO2 both at RB and UB sites but underestimates significantly the concentration especially during the cold season (FB=-54.4% over 2009).

Overall, for O3, the reproduction of the daily temporal variability is very good both at rural (R=0.78) and urban sites (R=0.77). The model reaches its lowest FB in summer (15.8%). Over the year, the modelled values present a systematic positive bias which is higher at urban (FB=28.6%) than at rural sites (19.8%). This tendency could be linked to the underestimation of the NO2 concentrations previously mentioned especially at urban sites.

For the PM10, at UB stations, the correlation takes its highest value during summer and autumn (0.46 and 0.48 respectively) and its lowest at spring (0.41). Inversely, the FB is lower in warmer seasons (-1.4% at spring time) than in winter (-30.5%). At RB site, the model performs better in terms of correlation (0.60) and tends, by opposition to the urban sites, to overestimate the concentration (FB=8.1% against -14.0% at UB on average over 2009).

For PM2.5, the behaviour is similar to PM10. However, we note a higher R value over the year both at UB sites (0.54) and RB sites (0.61) than for PM10. At UB sites, CHIMERE performs better in autumn (0.56) than in summer (0.40). The highest R is observed at RB sites during the winter (0.69). The FB is very low during the summer at UB stations (1.8%) and negative during the winter (-11.9%). At RB sites the FB is always positive and the maximum is observed at spring time (28.9%) and the minimum at winter time (6.5%). We underline that CHIMERE gives, over the year, a good performance concerning the reproduction of PM2.5 concentrations (FB=4.9%).

Table 6 : Selected statistical indicators calculated for NO2, O3, PM10, PM2.5, at UB AIRBASE stations; and sulphate, total nitrate and total ammonia at EMEP stations (grey lines)

Pollutant	Nb stations	Obs mean	Mod mean	R	RMSE	FB
NO2	770	13.2	8.2	0.61	8.4	-54.4
O3	586	23.6	29.5	0.77	9.8	28.5
PM10	677	29.3	22.8	0.42	21.9	-14.0
PM2.5	267	17.5	16.4	0.54	12.6	4.9
Sulphate	37	0.7	0.9	0.48	0.6	27.6
Total Nitrate	26	0.6	0.4	0.57	0.6	-57.8
Total Ammonia	14	1.5	1.4	0.60	1.1	-7.3

PM10, PM2.5 and PM speciation data are available on several EMEP sites. As previously observed with the Airbase RB stations, CHIMERE overestimates the PM10 (FB=19.9%) and PM2.5 (FB=20.1%) concentrations at the EMEP stations. A strong inter-seasonal variability is observed with a minimum FB during the winter (7.1% for PM10 and 0.6% for PM2.5). The highest correlation coefficient is found during the winter (0.55 for PM10) and is good for PM2.5 (0.69).

Concerning the secondary inorganic aerosols, an inter-seasonal variation is also noted. For sulphate, the model performs rather well during the summer (FB=7.1%) but strongly overestimates the concentration at spring time (FB=41.0). Nitrates are underestimated along the year but a rather high correlation value is noted during the winter (0.68). The total nitrate concentration is much better reproduced with R>0.6 over the year except during the summer (0.17). The underestimation of nitrates is due to the missing process of coarse nitrate production (Hodzic et al., 2006). Along with sulphate, ammonium appears to be the SIA which is the best reproduced by CHIMERE. The FB is rather low and indicates a slight overestimation during the winter (7.7%) and an underestimation during the summer (-5.9%). The total ammonia is nicely reproduced by CHIMERE with a low negative bias observed during the spring (FB=4.0%) and autumn (FB=-1.5%) seasons. The performance is worse during the summer where the model is underestimating the most (FB=-21.2%).

5.3 Spatial patterns of NO2, PM2.5 and PM10

Figure 10, Figure 11 and Figure 12 provide an overall picture of the CHIMERE performances respectively for NO2, PM10 and PM2.5 in 2009.

Clearly, the slight underestimation at backgound sites is displayed for NO2. For PM10 and PM2.5 the background concentrations are in good agreement with observations in most of the western part of Europe. In the east part of Europe, problems remain in some countries like Poland, Czech Republic and Slovakia, Bulgaria with a strong underestimation of PM concentrations. These problems are probably related to underestimated emission inventories.

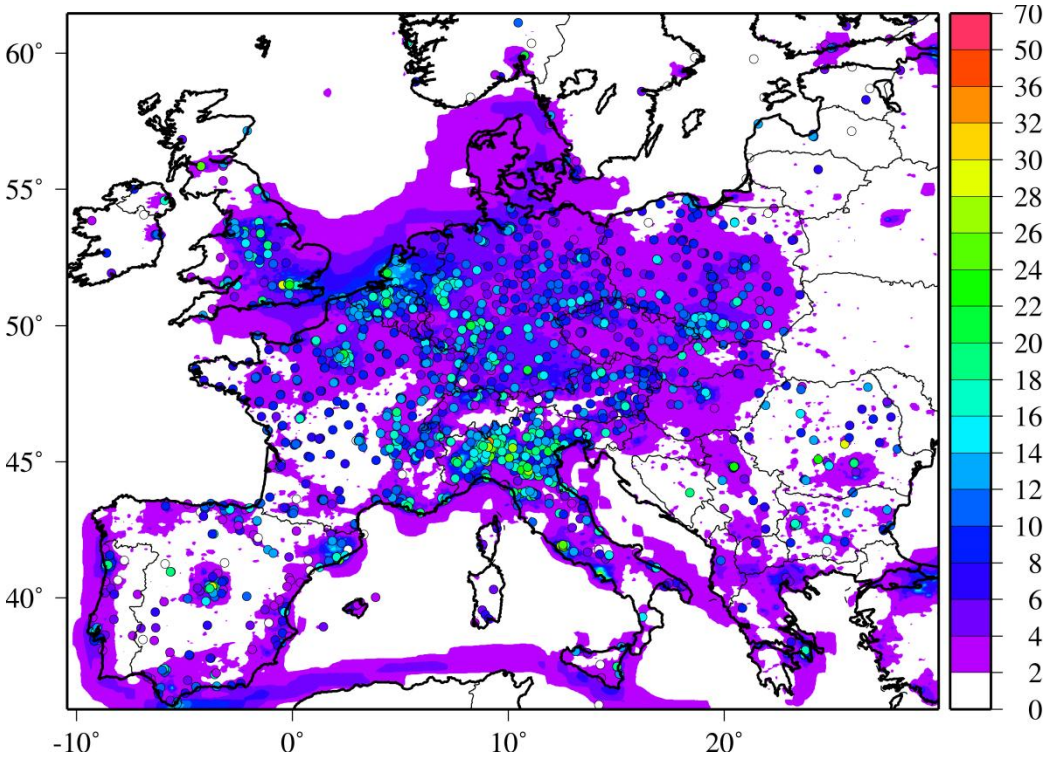

Figure 10 : NO2 concentration annual fields for urban, suburban and rural stations (ppb) – Coloured circles are the observations

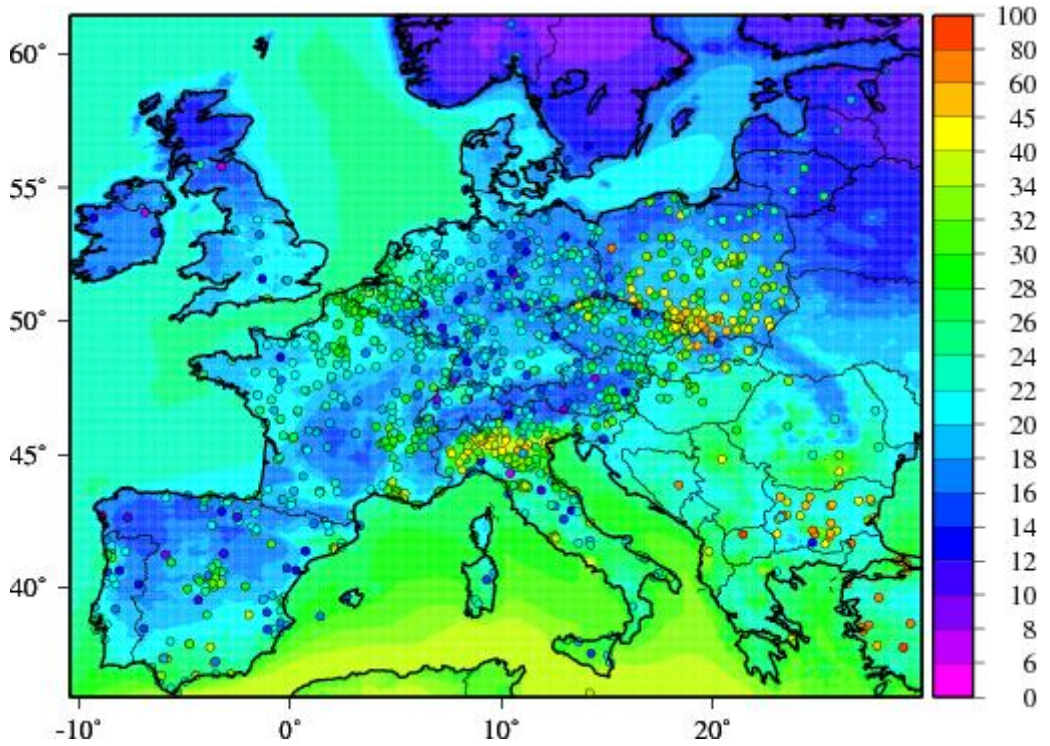

Figure 11 : PM10 concentration annual fields for urban, suburban and rural stations (µg/m^3) – Coloured circles are the observations

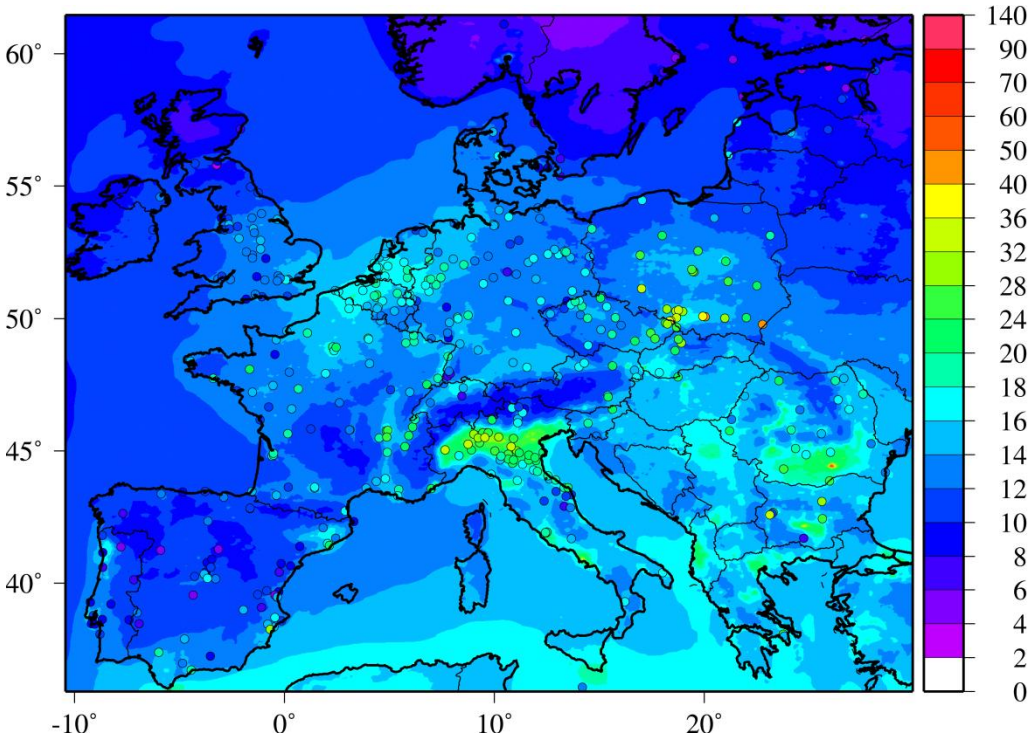

Figure 12 : PM2.5 concentration annual fields for urban, suburban and rural stations (µg/m^3) – Coloured circles are the observations

5.4 Added value of the high resolution

As expected, at rural sites, the 7km resolution simulation is consistent with the 50km outputs, the differences are very low. A significant increment is found for PM10 and NO2 between the 7km and the 50km resolution run for urban and suburban stations (Figure 13). Consistently, the observations at traffic sites cannot be reproduced by the model, a remaining increment needs to be added. For O3, a decrement is found from the 50 km to the 7km simulation, consistent with the titration effect in urban areas.

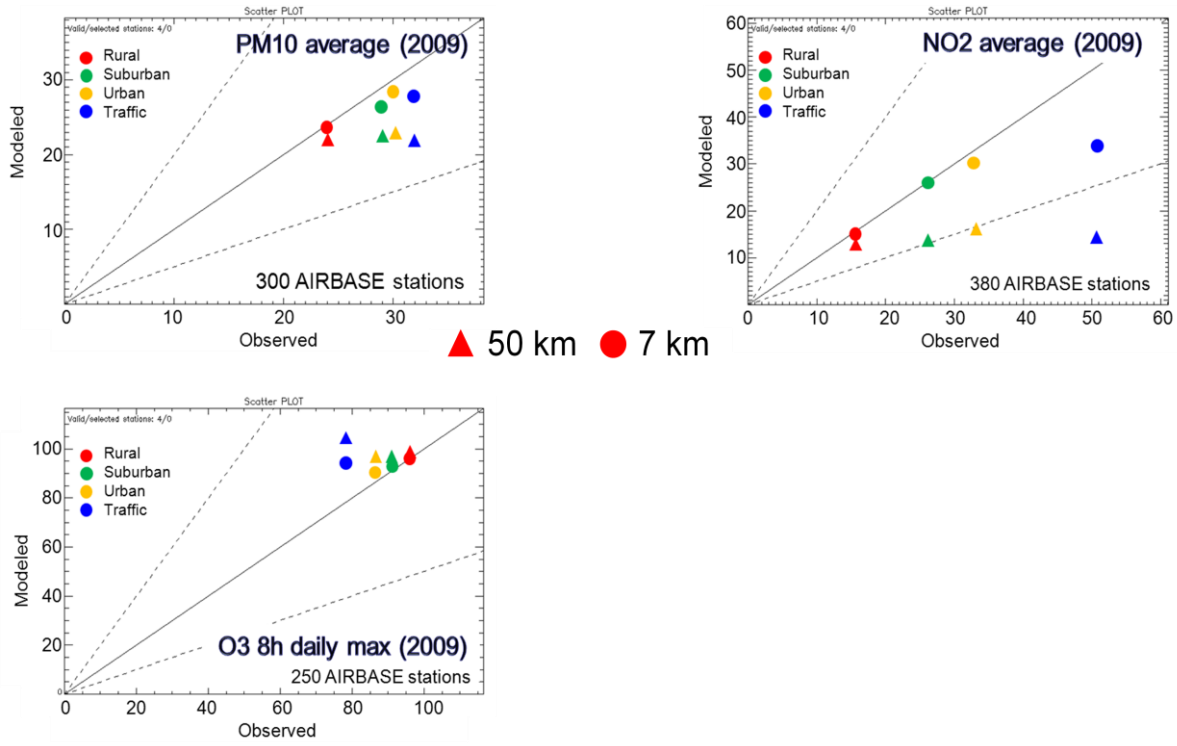

Figure 13 : Added value of the high resolution simulation (7km) compare to the coarse simulation (50km) for different types of sites

6 Conclusion

The CHIMERE model designed for EC4MACS is described in this report. The main improvements of CHIMERE focussed on the meteorology (Kz and wind speed corrections), the vertical resolution (add of a thin first layer, 20 m, at the ground level) and the emissions (improvement of the spatialisation and temporal distribution of SNAP2 emissions).

A comprehensive evaluation of the CHIMERE model was conducted for the year 2009.The performance of the model is varying according the type of stations and the time of year. It reproduces the daily NO2 variability along the year but underestimate significantly the concentration especially during the cold season.

The model reproduces nicely the day to day O3 variation similarly at urban and rural sites with an overestimation which is higher during the winter at urban sites. CHIMERE gives an overall satisfactory performance concerning the reproduction of the PM10 (FB=-14%) and a good performance concerning the reproduction of PM2.5 concentrations (FB=4.9%). For the sulphate, the model performs rather well during the summer (FB=7.1%) but overestimates the concentrations at spring time (FB=41.0%). The total nitrate concentration is much better reproduced than nitrate stand alone with high R over the year (R>0.6). For total nitrate, the model

underestimates the observations. Finally, the total ammonia is better reproduced by the model in spring (FB=4.0%) and autumn (FB=-1.5%) whereas the model performance is lower during the summer (FB=-21.2%).

The high resolution simulation improves the CHIMERE performances at urban stations for PM and NO2. This statement validates the use of CHIMERE to design a downscaling methodology that will be implemented in GAINS in the follow-up step of the EC4MACS project.

Acknowledgments

This project is funded by the ECMACS project (EU LIFE) and the French ministry of Ecology. We thank the DG JRC (Ph. Thunis, K. Cuvelier) for their support on the data analysis. Guido Pirovano (RSE) is also acknowledged for his technical and scientific support. The development of CHIMERE is made in close collaboration with LMD-IPSL/CNRS (Laurent Menut and Dmitry Khvorostyanov).

REFERENCES

Amann, M., Imrich Bertok, Jens Borken-Kleefeld, Janusz Cofala, Chris Heyes, Lena Höglund-Isaksson, Zbigniew Klimont, Binh Nguyen, Maximilian Posch, Peter Rafaj, Robert Sandler, Wolfgang Schöpp, Fabian Wagner, Wilfried Winiwarter, Cost-effective control of air quality and greenhouse gases in Europe: Modeling and policy applications, *Environmental Modelling & Software*, Volume 26, Issue 12, December 2011, Pages 1489-1501, ISSN 1364-8152, 10.1016/j.envsoft.2011.07.012, **2011**.

Appel, K. W., Robert C. Gilliam, Neil Davis, Alexis Zubrow, Steven C. Howard, Overview of the atmospheric model evaluation tool (AMET) v1.1 for evaluating meteorological and air quality models*, Environmental Modelling & Software*, Volume 26, Issue 4, April 2011, Pages 434-443, ISSN 1364-8152, 10.1016/j.envsoft.2010.09.007, **2011**.

Bessagnet, B., A. Hodzic, R. Vautard, M. Beekmann, S. Cheinet, C. Honoré, C. Liousse, L. Rouil, Aerosol modeling with CHIMERE—preliminary evaluation at the continental scale, *Atmospheric Environment*, Volume 38, Issue 18, June 2004, Pages 2803-2817, ISSN 1352-2310, 10.1016/j.atmosenv.2004.02.034, **2004**.

Bessagnet B., L.Menut, G.Curci, A.Hodzic, B.Guillaume, C.Liousse, S.Moukhtar, B.Pun, C.Seigneur, M.Schulz Regional modeling of carbonaceous aerosols over

Europe - Focus on Secondary Organic Aerosols, *Journal of of Atmospheric Chemistry*, 61, 175-202, **2009**.

Bessagnet B., L.Menut, G.Aymoz, H.Chepfer and R.Vautard, Modelling dust emissions and transport within Europe: the Ukraine March 2007 event, *Journal of Geophysical Research - Atmospheres,* 113, D15202, doi:10.1029/2007JD009541, **2008**.

Bicheron, P. et al. Geolocation assessment of 300m resolution MERIS GLOBCOVER ortho-rectified products. In Proceedings of MERIS/AATSR Colloque, Frascati, **2008**.

Bowman, F.m., Odum, J.R., Seinfeld, J.H., Pandis, S.N.: Mathematical model for gas-particle parttioning of secondary organic aerosols. *Atmos. Environ*. 31, 3921–3931 ,**1997**.

Cheinet, S. The parameterization of clear and cloudy convective boundary layers. Ph.D. Thesis, Ecole Polytechnique, Paris, France, **2002**.

Colella, P. and Woodward, P. R. The piecewise parabolic method (PPM) for gas-dynamical simulations. *Journal of Computational Physics*, 11:38–39, **1984**.

Fisher, P., Kukkonen, J., Piringer, M., Rotach, M. W., and Schatzmann, M.: Meteorology applied to urban air pollution problems: concepts from COST 715, *Atmos. Chem. Phys. Discuss*., 5, 7903-7927, doi:10.5194/acpd-5-7903-2005, **2005**.

Gelbard, F., Seinfeld, J.H., Simulation of multicomponent aerosol dynamics. Journal of colloid and Interface Science 78, 485–501, **1980**.

Giglio, L., Randerson, J. T., van der Werf, G. R., Kasibhatla, P. S., Collatz, G. J., Morton, D. C., and DeFries, R. S.: Assessing variability and long-term trends in burned area by merging multiple satellite fire products, *Biogeosciences*, 7, 1171-1186, doi:10.5194/bg-7-1171-2010, **2010**.

Ginoux, P., Chin, M., Tegen, I., Prospero, J.M., Holben, B., Dubovik, O., Lin, S.-J., Sources and distributions of dust aerosols simulated with the GOCART model. *Journal of Geophysical Research* 106, 20,255–20,273, **2001**.

Griffin,R.J., Cocker, E.R., Flagan,R.C., Seinfeld, J.H.: Organic aerosol formation from the oxidation of biogenic hydrocarbons. *J. Geophys. Res*. 104, 3555–3567 ,**1999**.

Guenther, A., Karl, T., Harley, P., Wiedinmyer, C., Palmer, P., Geron, C., 2006. Estimates of global terrestrial isoprene emissions using MEGAN (Model of Emissions of Gases and Aerosols from Nature). Atmos. Chem. Phys. 6, 31813210, **2006**.

Hodzic, A., B. Bessagnet, R. Vautard, A model evaluation of coarse-mode nitrate heterogeneous formation on dust particles, *Atmospheric Environment*, Volume 40, Issue 22, July 2006, Pages 4158-4171, ISSN 1352-2310, 10.1016/j.atmosenv.2006.02.015, **2006**.

Hov, O., Stordal, F., Eliasen, A., Photochemical oxidant control strategies in Europe: a 19 day case study using a Lagrangian model with chemistry. NILU TR5/95, **1985**.

Jiménez, P. A., Dudhia, J. Improving the Representation of Resolved and Unresolved Topographic Effects on Surface Wind in the WRF Model. *J. Appl. Meteor. Climatol*., 51, 300–316, **2012**.

Kastner-Klein, P., Rotash, M. Mean flow and turbulence characteristics in an urban roughness sublayer*, Boundary-Layer Meteorology*, Volume 111, Number 1, 55-84, **2004**.

Kroll, J.H., Ng, N.L., Murphy, S.M., Flagan, R.C., Seinfeld, J.H.Secondary organic aerosol formation from isoprene photooxidation. Environ. Sci. Technol. 40, 1869–1877, **2006**.

Lattuati, M., Impact des !emissions Europ!eennes sur le bilan d'ozone troposh!erique "a l'interface de l'Europe et de l'Atlantique Nord: apport de la mod!elisation lagrangienne et des mesures en altitude. Doctaral *Thesis*, Universit!e P&M Curie, Paris, **1997**.

Louis, J., Tiedke, M., and Geleyn, J. A short history of the pbl parametrization at ecmwf. ECMWF Workshop on Planetary Boundary Layer parametrization, pages 59–80, **1982**.

Madronich, S., Flocke, S., The role of solar radiation in atmospheric chemistry. In: Boule, P. (Ed.), *Handbook of Environmental Chemistry*. Springer, Heidelberg, pp. 1–26, **1998**.

Menut, L., Goussebaile, A., Bessagnet, B., Khvorostiyanov, K. Ung, A. Impact of realistic hourly emissions profiles on air pollutants concentrations modelled with CHIMERE, Atmospheric Environment, Volume 49, March 2012, Pages 233-244, ISSN 1352-2310, 10.1016/j.atmosenv.2011.11.057, **2012**.

Middleton, P., Stockwell, W. R., Carter, W. P., Agregation and analysis of volatile organic compound emissions for regional modelling. *Atmospheric Environment* 24,1107–1133, **1990**.

Monahan, E. C. In The Role of Air-Sea Exchange in Geochemical Cycling, chapter The ocean as a source of atmospheric particles, pages 129–163. Kluwer Academic Publishers, Dordrecht, Holland, **1986**.

Nenes, A., Pilinis, C., Pandis, S.N., ISORROPIA: a new thermodynamic model for inorganic multicomponent atmospheric aerosols. Aquatic Geochemistry 4, 123–152, **1998**.

Odum, J.R., Jungkamp, T.P.W., Griffin, R.J., Forstner, J.L., Flagan, R.C., Seinfeld, J.H.: Aromatics, reformulated gasoline and atmospheric organic aerosol formation. *Environ. Sci. Technol*. 31, 1890–1897, **1997**.

Pay, M.T., Jiménez-Guerrero, P., Jorba, O., Basart, S., Querol, X., Pandolfi, M., Baldasano, J.M. Spatio-temporal variability of concentrations and speciation of particulate matter across spain in the caliope modeling system, *Atmospheric Environment*, doi: 10.1016/, j.atmosenv.2011.09.049, **2011**.

Pun, B., Seigneur, C., Lohman, K.: Modeling secondary organic aerosol via multiphase partitioning with molecular data. *Environ. Sci. Technol*. 40, 4722–4731, **2006**.

Raupach, M. R., 'A Wind-Tunnel Study of Turbulent Flow Close to Regularly Arrayed Roughness elements, *Boundary-Layer Meteorol*. 18, 373–397, **1980**.

Raupach,M. R.,Antonia R. A., and Rajagopalan S. 'Rough-Wall Turbulent Boundary Layers, *Appl. Mech. Rev*. 44, 1–25, **1991**.

Rotach, M. W.: 'Turbulence Close to a Rough Urban Surface, Part I: Reynolds Stress, *Boundary-Layer Meteorol*. 65, 1–28, **1993a**.

Rotach, M. W.: 'Turbulence Close to a Rough Urban Surface, Part II: Variances and Gradients, *Boundary-Layer Meteorol*. 66, 75–92, **1993b**.

Schmidt, H., Derognat, C., Vautard, R., Beekmann, M. A comparison of simulated and observed ozone mixing ratios for the summer of 1998 in western Europe. *Atmospheric Environment* 35, 6277–6297, **2001**.

Schulz, M., Textor, C., Kinne, S., Balkanski, Y., Bauer, S., Berntsen, T., Berglen, T., Boucher, O., Dentener, F., Guibert, S., Isaksen, I.S.A., Iversen, T., Koch, D., Kirkevå g, A., Liu, X., Montanaro, V., Myhre, G., Penner, J.E., Pitari, G., Reddy, S., Seland, O., Stier, P., Takemura, T., Radiative forcing by aerosols as derived from the AeroCom present-day and pre-industrial simulations. *Atmos. Chem. Phys.* 6, 5225–5246, **2006**.

Siedlecki, M, Urban – rural wind speed differences in Lodz, University of Lodz, Poland. Online resource.

Solazzo, E., Di Sabatino, S., Aquilina, N., Dudek, A., Britter, R., Coupling Mesoscale Modelling with a Simple Urban Model: The Lisbon Case Study, *Boundary-Layer Meteorol* 137:441–457, DOI 10.1007/s10546-010-9536-6, **2010**.

Thunis, P., L. Rouil, C. Cuvelier, R. Stern, A. Kerschbaumer, B. Bessagnet, M. Schaap, P. Builtjes, L. Tarrason, J. Douros, N. Moussiopoulos, G. Pirovano, M. Bedogni Analysis of model responses to emission-reduction scenarios within the citydelta project *Atmospheric Environment*, 41 (1) pp. 208–220, **2007**.

Troen, I. and Mahrt, L. A simple model of the atmospheric boundary layer: Sensitivity to surface evaporation. *Bound.-Layer Meteorol*., 37:129–148, **1986**.

Vautard, R., Bessagnet, B., Chin, M., Menut, L. On the contribution of natural Aeolian sources to particulate matter concentrations in Europe: Testing hypotheses with a modelling approach, *Atmospheric Environment*, Volume 39, Issue 18, June 2005, Pages 3291-3303, ISSN 1352-2310, 10.1016/j.atmosenv.2005.01.051, **2005**.

Vestreng, V., Review and revision of emission data reported to CLRTAP. EMEP Status report, **2003**.

Warren, D.R., Nucleation and growth of aerosols. Thesis of the California Institute of Technology, Pasadena, **1986**.

Zhang, Y., Huang, J.-P., Henze, D.K., Seinfeld, J.H.: Role of isoprene in secondary organic aerosol formation on a regional scale. *J. Geophys. Res*. 112, D20207 doi:10.1029/2007JD008675, **2007**.